Three-dimensional gap solitons in Bose-Einstein condensates supported by one-dimensional optical lattices

A. Muñoz Mateo[1], V. Delgado[1], and Boris A. Malomed[2]
[1]*Departamento de Física Fundamental II, Universidad de La Laguna, 38206 La Laguna, Tenerife, Spain and*
[2]*Department of Physical Electronics, School of Electrical Engineering, Faculty of Engineering, Tel Aviv University, Tel Aviv 69978, Israel*

(Dated: 11 June 2010)

We study fundamental and compound gap solitons (GSs) of matter waves in one-dimensional (1D) optical lattices (OLs) in a three-dimensional (3D) weak-radial-confinement regime, which corresponds to realistic experimental conditions in Bose-Einstein condensates (BECs). In this regime GSs exhibit nontrivial radial structures. Associated with each 3D linear spectral band exists a family of fundamental gap solitons that share a similar transverse structure with the Bloch waves of the corresponding linear band. GSs with embedded vorticity m may exist *inside* bands corresponding to other values of m. Stable GSs, both fundamental and compound ones (including vortex solitons), are those which originate from the bands with lowest axial and radial quantum numbers. These findings suggest a scenario for the experimental generation of robust GSs in 3D settings.

PACS numbers: 03.75.Lm, 05.45.Yv, 42.65.Tg

I. INTRODUCTION

A ubiquitous tool for the control of collective excitations in Bose-Einstein condensates (BECs) is provided by optical lattices (OLs), which are induced by the interference of laser beams illuminating the condensate [1]. OLs are especially efficient in supporting matter-wave solitons. It has been predicted that two- and three-dimensional (2D and 3D) OLs can stabilize solitons against collapse [2]. OLs acting in the combination with repulsive interactions can give rise to diverse species of gap solitons (GSs), in one dimensional (1D) [3, 4] and multidimensional [5, 6] geometries. Quasistable GSs were created in the ^{87}Rb condensate loaded into a cigar-shaped trap incorporating an axial OL [7]. Extended states, built as segments of nonlinear Bloch waves trapped in the OL, were also reported [8].

Most theoretical studies of GSs have been carried out in the quasi-1D regime, assuming that the transverse confinement is tight enough to reduce the wave function in the transverse plane to the ground state of the corresponding 2D harmonic oscillator (HO) [9, 10]. In this case, the description of the relevant dynamics amounts to the 1D Gross-Pitaevskii equation (GPE) in the axial direction, which follows from the underlying 3D equation after averaging out the radial (transverse) degree of freedom. Since in the quasi-1D regime the radial quantum $\hbar\omega_\perp$ is the largest energy scale of the system, GSs cannot decay by exciting higher-order radial modes, being therefore particularly stable. However, the creation of genuine quasi-1D settings, strongly squeezed in the radial direction —for instance, those realizing the Tonks-Girardeau gas [11]— is a challenging experimental problem. The settings used in experiments with GSs [1, 7, 8] actually correspond to the weak transverse confinement (see details in Sec. IV).

In this work we aim to predict matter-wave GSs in the regime of the weak radial confinement, characterized by a recoil energy of the axial OL, E_R, comparable to $\hbar\omega_\perp$. While this regime is most relevant to the experiment, the formation of GSs under these conditions was not yet studied theoretically. For instance, $E_R/\hbar\omega_\perp = 1$ corresponds to the ^{87}Rb condensate, with s-wave scattering length $a_s = 5.29$ nm, confined by the combination of the transverse trapping frequency $\omega_\perp/2\pi = 240$ Hz and axial OL of period $d = 1.55$ μm (physical results given in this article correspond to this typical setting). In this regime, the axial GS structure may readily excite higher modes of the radial confinement; hence the 3D character of the dynamics is essential and the 1D reduction cannot be used. The situation is somewhat similar to that for quasi-1D GSs, which were predicted, in the framework of the density-functional description, in fermionic superfluids [12]. In that case, the underlying Fermi distribution implies the filling of many transverse energy levels.

While there are models that generalize the 1D GPE by taking into account small deviations from the one-dimensionality [9, 10], we consider the setting in which the axial and radial directions are equally important and inseparable; hence the use of the full 3D equation is necessary. We demonstrate that stable solitons, which are true gap modes in terms of the underlying 3D band-gap structure, exist in this regime, suggesting possibilities for the creation of robust 3D solitons. This objective is of principal significance because, thus far, no truly 2D or 3D matter-wave solitons, nor their counterparts in optical media with the Kerr nonlinearity, have been created, in spite of many theoretical predictions [13]. We also find solitons *inside* the bands, which may exist due to the difference in the azimuthal index between the soliton and the band.

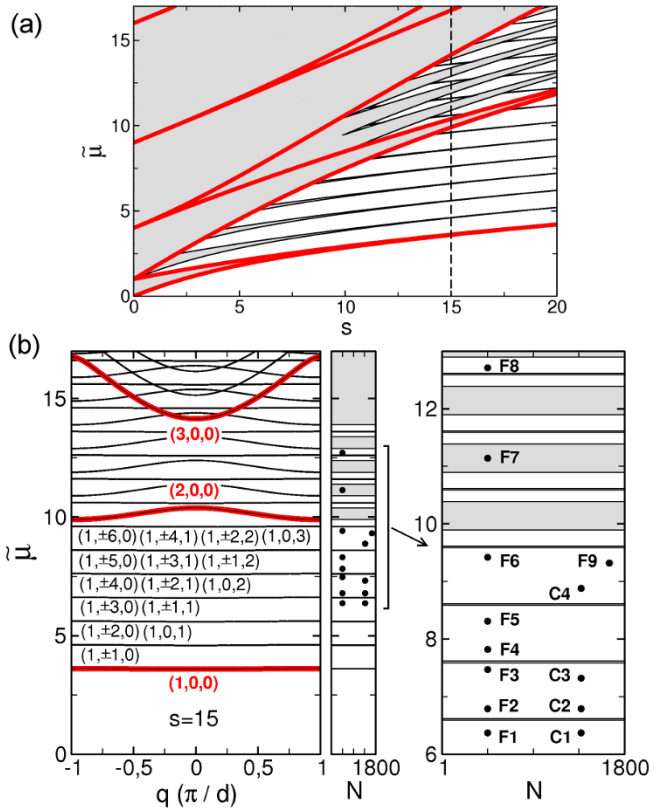

FIG. 1: (Color online) The band-gap structure, produced by the linearized GPE, with equal axial and transverse energies, $E_R/\hbar\omega_\perp = 1$ (white areas are gaps). The normalized chemical potential is shown vs the scaled lattice depth, s (a), and as a function of quasimomentum q for $s = 15$ (b). The right-hand panels in (b) indicate the location of the GSs displayed in this paper. Sets (n, m, n_r) represent the quantum numbers, and the bold red curves depict the band-gap structure in the 1D model.

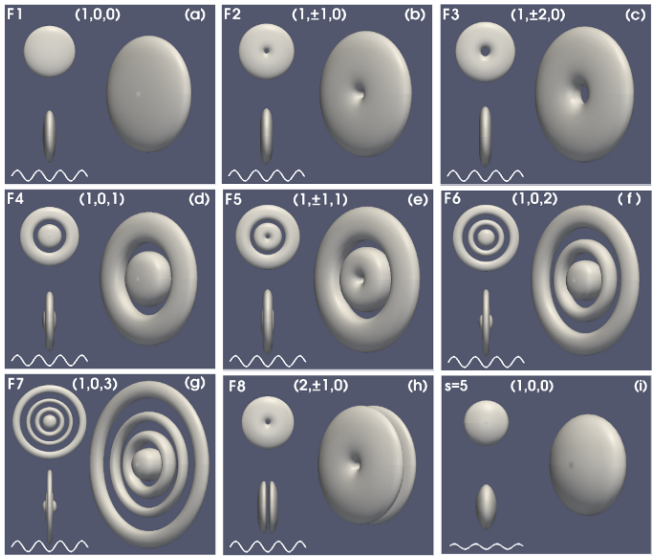

FIG. 2: (Color online) Isosurfaces of the atomic density, taken at 10% of the maximum value, for GSs corresponding to points F1–F8 in Fig. 1(b). Panel (i) depicts a GS in a weaker lattice, with $s = 5$. The respective quantum-number sets, (n, m, n_r), are indicated in each panel. The length scale of the left part in each panel (reduced to 45% in comparison with the image on the right) is gauged by the OL period.

II. THREE-DIMENSIONAL GAP SOLITONS

The 3D GPE, with the radial-HO and axial potentials, $V_\perp(\mathbf{r}_\perp) = (M/2)\omega_\perp^2 r_\perp^2$ and $V_z(z) = sE_R \sin^2(\pi z/d)$, is

$$i\hbar\psi_t = \left[-\left(\hbar^2/2M\right)\nabla^2 + V_\perp(\mathbf{r}_\perp) + V_z(z) + gN|\psi|^2\right]\psi, \quad (1)$$

where N and M are the atomic number and mass, $g \equiv 4\pi\hbar^2 a_s/M$, d and s are the period and depth of the OL, the recoil energy is $E_R = (\pi\hbar)^2/(2Md^2)$, and the norm of the wave function is 1 [14].

Figure 1(a) displays the scaled shifted chemical potential, $\widetilde{\mu} \equiv (\mu - \hbar\omega_\perp)/E_R$, of the noninteracting 3D condensate ($g = 0$) with $E_R/\hbar\omega_\perp = 1$, as a function of the OL strength s. In the plot, bandgaps separate shaded Bloch bands. For the sake of comparison, the band-gap diagram obtained from the corresponding 1D equation is also shown (bold red lines). Since the energy levels of the radial HO are $E = (2n_r + |m| + 1)\hbar\omega_\perp$, where $n_r = 0, 1, 2, \ldots$ and $m = 0, \pm1, \pm2, \ldots$ are the radial and azimuthal quantum numbers, the excitation of transverse modes gives rise to a series of replicas of 1D Bloch bands, shifted up in the energy by multiples of $\hbar\omega_\perp/E_R$. In what follows, we present most of our results for a strong OL with $s = 15$, which corresponds to the dashed vertical line in Fig. 1(a). The respective spectrum is shown in Fig. 1(b), which displays $\tilde{\mu}$ as a function of quasimomentum q in the first Brillouin zone. The 3D bands are characterized by quantum-number sets (n, m, n_r), where $n = 1, 2, 3, \ldots$ is the band index of the corresponding 1D axial problem. As in Fig. 1(a), the superimposed bold red lines represent the results generated by the corresponding 1D equation. As indicated in Fig. 1(b), the lowest band corresponds to $(n, m, n_r) = (1, 0, 0)$. The next two bands, with numbers $(1, \pm1, 0)$, have equal chemical potentials, being replicas of the lowest band shifted upward by $\hbar\omega_\perp/E_R$. Likewise, the next three bands, with numbers $(1, \pm2, 0)$ and $(1, 0, 1)$, are shifted by $2\hbar\omega_\perp/E_R$ and so on. Dots in the right-hand panels in Fig. 1(b) indicate the location of the GSs that we consider in this paper, with the horizontal axes indicating the number of ^{87}Rb atoms in each nonlinear state.

GS solutions have been obtained as numerical solutions of the stationary version of Eq. (1), using the Newton continuation method with the Laguerre-Fourier functional basis. In Fig. 2 we display a set of solutions for GSs which

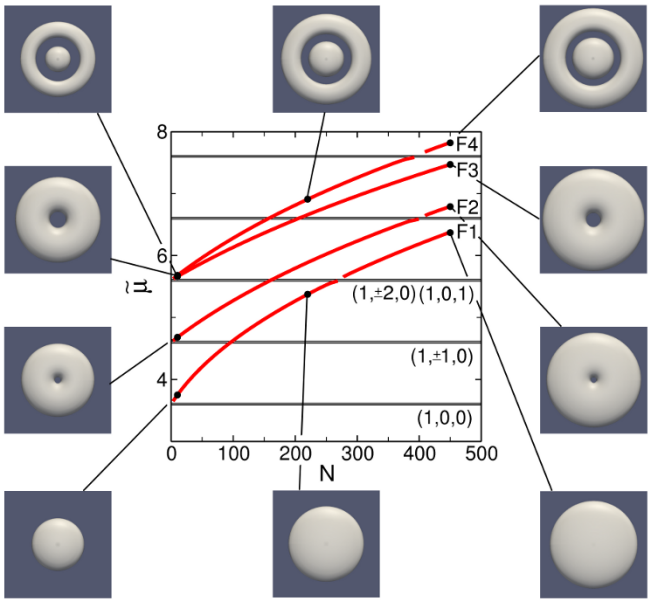

FIG. 3: (Color online) The $\widetilde{\mu}(N)$ curves representing the four lowest-lying GS families. The inserted panels display the solitons at marked points. The field of view in each panel is $4.6\,\mu\mathrm{m} \times 4.6\,\mu\mathrm{m}$, in terms of the ^{87}Rb condensate.

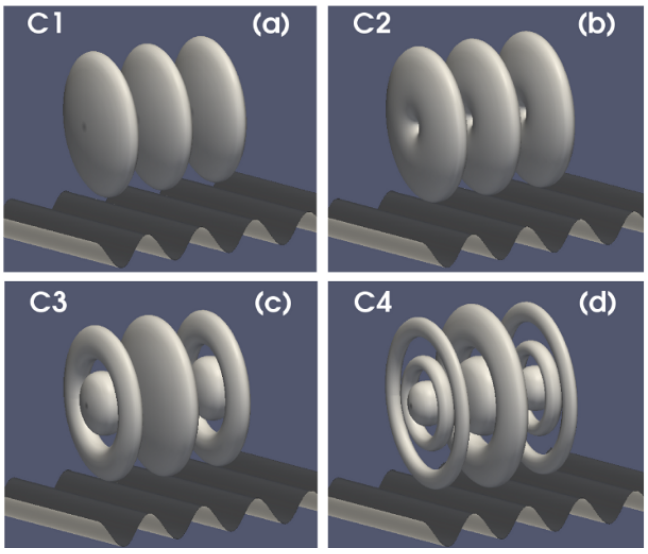

FIG. 4: (Color online) Gap-soliton complexes corresponding to points C1–C4 in Fig. 1(b). The underlying 1D lattice potential is also shown.

correspond to points F1–F8 in Fig. 1(b). Stable GSs correspond to $n_r = 0$ [panels (a)–(c) and (h)]. In addition, Fig. 2(i) displays an example of a loosely bound but also stable GS supported by a weaker OL, with $s = 5$. The parameters are adjusted to $N = 450$ atoms [$N = 350$ in Fig. 2(i)]; in Ref. [7], the GS had $\simeq 250$ atoms. The right-hand image in each panel is a perspective image, while the top and bottom left plots are axial and lateral views.

As shown in Fig. 3, GS families are represented by $\widetilde{\mu}(N)$ curves, each approaching a certain band at $N \to 0$, whose set (n, m, n_r) is used to label the families. As N increases, the size of the GSs increases too, keeping a characteristic soliton structure. The GS with the lowest chemical potential, of type $(1, 0, 0)$, which corresponds to point F1 in Fig. 1(b), is shown in Fig. 2(a). GSs of this type are disk-shaped objects localized within a single cell of the axial OL. While the radial shape of this GS approaches the ground state of the corresponding HO at $N \to 0$, the contribution of radially excited states becomes more pronounced with the increase of N, making the GS a fully 3D mode. In particular, point F1 in Fig. 1(b), with $\widetilde{\mu} = 6.37$, corresponds to $\mu = 7.37\hbar\omega_\perp$ in physical units, which is *much larger* than the radial-excitation quantum, $\hbar\omega_\perp$. The decomposition of this GS over the basis of radial HO modes yields a mixture of states $n_r = 0, 1$, and 2, with respective weights $76\%, 22\%$, and 2%

As per azimuthal index m, the GSs in the $(1, 1, 0)$ and $(1, 2, 0)$ families carry vorticities 1 and 2; see Figs. 2 and 3. (The vorticity may also be embedded into solitons in the case of the tight transverse confinement, with $\hbar\omega_\perp \gg E_R$ [10], as well as into GSs supported by the OL in the 2D geometry [6].) The GSs corresponding to $n_r \geq 1$ feature a complex radial structure, composed of many HO modes. Nevertheless, these solitons exhibit a set of zero-density rings reminiscent of the HO wave functions with the respective values of n_r; see Figs. 2(d), 2(f) and 2(g) for $n_r = 1, 2$, and 3.

The higher-order ($n = 2$) band of the axial potential gives rise to GS families of types $(2, \pm 1, 0)$. As seen in Fig. 2(h), they exhibit two major peaks in the axial direction with a node between them, all squeezed into a *single* lattice cell (in the 1D GPE, solitons of this type are known as subfundamental GSs [4]). On the other hand, because band gaps emerging at large values of the chemical potential are very narrow, no GS of type $(2, 0, 0)$ exists here, as it is not able to place itself within the corresponding narrow gap. It is worth noting, too, that GSs of the $(1, 0, 3)$ and $(1, 1, 2)$ types are found *inside* the $(2, 1, 0)$ and $(2, 0, 0)$ Bloch bands, respectively [the former case corresponds to point F7 in Figs. 1(b) and 2(g)], which is possible because modes with different azimuthal numbers m do not mix. In fact, these may be understood as examples of "embedded solitons", whose chemical potential falls within linear bands. While they were studied in detail in 1D models [15], no example of multidimensional embedded solitons has been reported previously.

Fundamental gap solitons play an important role as elementary building blocks of higher order localized nonlinear structures [16]. Some examples of the latter, generated from the symmetric linear combination of three fundamental solitons, are shown in Fig. 4. The gap solitons displayed in Figs. 4(a) and 4(b), which are composed of

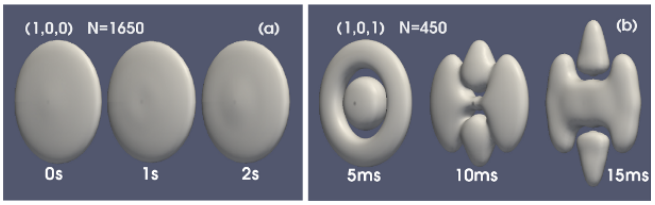

FIG. 5: (Color online) (a) The stable evolution of a GS of the $(1,0,0)$ type after the application of the perturbation. (b) The instability of the soliton of the $(1,0,1)$ type, from Fig. 2(d).

three identical $(1,0,0)$ and $(1,1,0)$ solitons, respectively, and correspond to points C1 and C2 in Fig. 1(b), have exactly the same chemical potentials as their respective elementary constituents ($\widetilde{\mu} = 6.37$ and 6.79) but contain approximately three times as many particles ($N = 1372$). The compound gap solitons in Figs. 4(c) and 4(d), which have the same particle content as the previous ones but are higher in the spectrum (points C3 and C4), are bound states of fundamental constituents of different types. The former is composed of one $(1,0,0)$ and two $(1,0,1)$ solitons, while the latter contains one $(1,0,1)$ and two $(1,0,2)$ fundamental solitons.

III. STABILITY

The stability of the GSs was tested by simulating their perturbed evolution. To this end, Eq. (1) was solved by the Laguerre-Fourier pseudospectral method, using the third-order Adams-Bashforth time-marching scheme. To include all potentially dangerous disturbances, we perturbed the GSs by simultaneously increasing the OL depth and decreasing its period, both by 2%, translating the OL in the axial direction by 2% of the lattice period, and applying a 2% quadrupole deformation to the transverse trapping potential. After waiting for $t = 1$ ms, the combined perturbation was removed, allowing the system to evolve for 2 s. The simulations demonstrate that the fundamental GSs of the $(1,0,0)$ and $(1,1,0)$ types remain stable, except in narrow regions close to edges of the corresponding band gaps. As a representative example, Fig. 5(a) displays the evolution of the soliton of the $(1,0,0)$ type, corresponding to point F9 in Fig. 1(b), which represents a GS built of 1650 atoms with $\mu = 10.3\hbar\omega_{\perp}$. While the latter is much greater than the transverse quantum $\hbar\omega_{\perp}$, the GS remains stable under the action of the 3D perturbations. The loosely bound GSs trapped in weaker OLs, such as the one in Fig. 2(i), are stable as well.

Although vortices with the $m = 2$ are usually unstable against splitting [17], they may be stable in trapped configurations [18]. We have found that the GS of type $(1,2,0)$ is stabilized by making it heavier: While it is unstable if built of $\lesssim 300$ atoms, the one shown in Fig. 2(c), which contains 450 atoms, is robust in the simulations. On the other hand, GSs with $n_r \geq 1$ (that is, those featuring the complex radial structure) are unstable against quadrupole perturbations. In particular, Fig. 5(b) displays the instability for the GS of type $(1,0,1)$, initiated by a very weak (0.1%) quadrupole deformation of the trapping potential, acting for 0.2 ms. GSs with $n = 2$ are also unstable, similar to the previously mentioned "subfundamental solitons" in 1D models [4]. Finally, the stability of GS complexes coincides with that of their fundamental constituents.

IV. CONCLUSION

Up to now, matter-wave GSs were actually created in shallow lattices ($s \simeq 0.7$), with a weak radial confinement ($E_R/\hbar\omega_{\perp} \simeq 44$) [7]. The respective linear spectrum does not exhibit true band gaps. This can be checked using the approximate dispersion relation for the lowest-energy band in the shallow OL, $E(q)/E_R = (qd/\pi - 1)^2 - \sqrt{4(qd/\pi - 1)^2 + s^2/16}$ [1]. As follows from this, the width of the lowest band, $E(1) - E(0) \simeq 0.83E_R$, is *much larger* than the gap, $\hbar\omega_{\perp} \simeq 0.027E_R$, which separates the replicas corresponding to higher values of azimuthal number m, and hence different Bloch bands overlap in this case. (For parameters of the experiment from Ref. [7], true gaps open up only at $s \geq 16$.) Therefore, the solitary modes obtained under such conditions are actually quasisolitons, decaying on a time scale of $\simeq 60$ ms [7]. The present results suggest possibilities for the creation of robust fundamental and compound GSs, including vortical ones, which place themselves in true band gaps. Simultaneously, this approach opens possibilities for creating truly multidimensional matter-wave solitons, which thus far have been elusive in experiments.

In addition to the BEC, the proposed scheme may be used for the creation of 3D "light bullets" of the GS type in self-defocusing optical media with the anomalous group-velocity dispersion. In that case, t and z in Eq. (1) play the roles of the transmission distance and reduced time [13]. The corresponding lattice cannot be created as a material structure, but it may be induced by a beating wave launched at a different wavelength, similar to the virtual grating used for the creation of optical GSs in 1D [19]. Thus far, no 3D solitons have been created in optical media.

V.D. acknowledges financial support from Ministerio de Ciencia e Innovación FIS2009-07890 (Spain). The work of B.A.M. was supported, in a part, by the German-Israel Foundation through grant No. 149/2006.

[1] O. Morsch and M. Oberthaler, Rev. Mod. Phys. **78**, 179 (2006).

[2] B. B. Baizakov, B. A. Malomed and M. Salerno, Europhys. Lett. **63**, 642 (2003); Phys. Rev. A **70**, 053613 (2004); J. Yang and Z. H. Musslimani, Opt. Lett. **28**, 2094 (2003); J. Yang, I. Makasyuk, A. Bezryadina, and Z. Chen, Stud. Appl. Math. **113**, 389 (2004); D. Mihalache *et al.*, Phys. Rev. E **70**, 055603(R) (2004).

[3] F. Kh. Abdullaev *et al.*, Phys. Rev. A **64,** 043606 (2001); I. Carrusotto, D. Embriaco, and G. C. La Rocca, *ibid.* 65, 053611 (2002).

[4] N. K. Efremidis and D. N. Christodoulides, Phys. Rev. A **67**, 063608 (2003); T. Mayteevarunyoo and B. A. Malomed, *ibid*. **74**, 033616 (2006); J. Cuevas, B. A. Malomed, P. G. Kevrekidis, and D. J. Frantzeskakis, *ibid*. **79**, 053608 (2009).

[5] B. B. Baizakov, V. V. Konotop and M. Salerno, J. Phys. B: At. Mol. Opt. Phys. **35**, 5105 (2002); P. J. Y. Louis, E. A. Ostrovskaya, C. M. Savage, and Y. S. Kivshar, Phys. Rev. A **67**, 013602 (2003); Z. Shi, J. Wang, Z. Chen, and J. Yang, Phys. Rev. A **78**, 063812 (2008).

[6] E. A. Ostrovskaya and Y. S. Kivshar, Phys. Rev. Lett. **93**, 160405 (2004); H. Sakaguchi and B. A. Malomed, J. Phys. B: At. Mol. Opt. Phys. **37**, 2225 (2004).

[7] B. Eiermann *et al.*, Phys. Rev. Lett. **92**, 230401 (2004).

[8] Th. Anker *et al.*, Phys. Rev. Lett. **94**, 020403 (2005); T. J. Alexander, E. A. Ostrovskaya, and Y. S. Kivshar, *ibid*. **96**, 040401 (2005).

[9] A. E. Muryshev *et al.*, Phys. Rev. Lett. **89**, 110401 (2002); L. D. Carr and J. Brand, *ibid*. **92**, 040401 (2004); M. Matuszewski, W. Królikowski, M. Trippenbach, and Y. S. Kivshar , Phys. Rev. A **73**, 063621 (2006); A. Muñoz Mateo and V. Delgado, Phys. Rev. A **75**, 063610 (2007); *ibid.* **77**, 013617 (2008); Ann. Phys. **324**, 709 (2009).

[10] L. Salasnich, A. Parola, and L. Reatto, Phys. Rev. A **65**, 043614 (2002); *ibid*. **66**, 043603 (2002); L. Salasnich, A. Cetoli, B.A. Malomed, and F. Toigo *ibid*. **75**, 033622 (2007); L. Salasnich, B. A. Malomed, and F. Toigo, Phys. Rev. A **76**, 063614 (2007).

[11] B. Paredes *et al.*, Nature **429**, 277 (2004).

[12] S. Adhikari and B. A. Malomed, Europhys. Lett. **79**, 50003 (2007); Physica D **238**, 1402 (2009).

[13] B. A. Malomed, D. Mihalache, F. Wise, and L. Torner, J. Optics B: Quant. Semicl. Opt. **7**, R53 (2005).

[14] R. Carretero-González, D. J. Frantzeskakis, and P. G. Kevrekidis, Nonlinearity **21**, R139 (2008).

[15] J. Yang, B. A. Malomed, and D. J. Kaup, Phys. Rev. Lett. **83**, 1958 (1999); A. R. Champneys, B. A. Malomed, J. Yang, and D. J. Kaup, Physica D **152-153**, 340 (2001); J. K. Yang, Phys. Rev. Lett **91**, 143903 (2003); X. S. Wang, Z. G. Chen, J. D. Wang, and J. K. Yang, , *ibid*. **99**, 243901 (2007).

[16] M. Matuszewski, E. Infeld, B. A. Malomed, and M. Trippenbach, Phys. Rev. Lett. **95**, 050403 (2005); Y. Zhang and B. Wu, *ibid.* **102**, 093905 (2009); J. D. Wang, J. K. Yang, T. J. Alexander, and Y. S. Kivshar, Phys. Rev. A **79**, 043610 (2009).

[17] A. Muñoz Mateo and V. Delgado, Phys. Rev. Lett. **97**, 180409 (2006); J. A. Huhtamäki *et al*., *ibid.* **97**, 110406 (2006); K. Gawryluk, M. Brewczyk, and K. Rzazewski, J. Phys. B: At. Mol. Opt. Phys. **39**, L225 (2006).

[18] H. Pu *et al*., Phys. Rev. A **59**, 1533 (1999).

[19] G. Van Simaeys, S. Coen, M. Haelterman, and S. Trillo, Phys. Rev. Lett. **92**, 223902 (2004).